

## **Analysis of carbon erosion/deposition in the private flux region of the JET MKII-HD divertor using QMB technique**

H.G. Esser<sup>1</sup>, A. Kreter<sup>1</sup>, V. Philipps<sup>1</sup>, A.M. Widdowson<sup>2</sup>, J.P. Coad<sup>2</sup>  
and JET EFDA contributors\*

<sup>1</sup> *Institut für Energieforschung – Plasmaphysik, Forschungszentrum Jülich GmbH, EURATOM-  
Association, Trilateral Euregio Cluster, D-52425 Jülich, Germany*

<sup>2</sup> *UKAEA/EURATOM Fusion Assoc., Culham Science Centre, Abingdon, UK*

\* *See the Appendix of M.L. Watkins et al., Fusion Energy 2006 (Proc. 21st Int. Conf. Chengdu,  
2006) IAEA, (2006)*

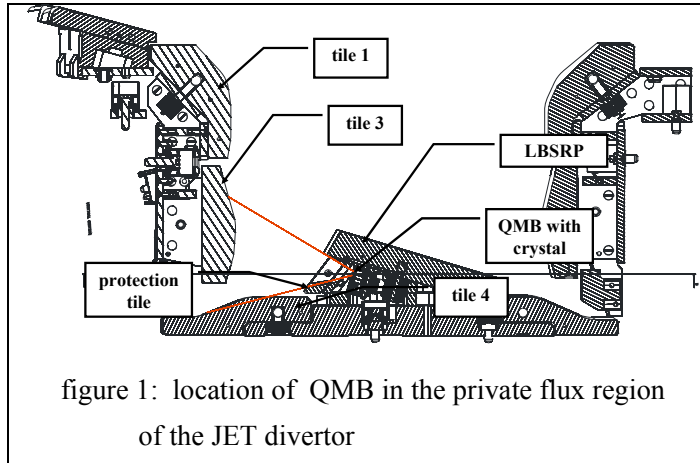
### **1. Introduction and motivation**

The qualification of plasma facing materials for the ITER divertor is a key issue in present fusion research. Erosion and redeposition of graphite and tritium accumulation in subsequently formed carbon layers on the target plates and in remote areas is one of the most critical questions associated with the life time of carbon fibre composites (CFCs) on the lower target plates of ITER. To study these effects in a time and space resolved mode a set of six Quartz Microbalance (QMB) systems was installed in the JET divertor in the shutdown 2004 at various poloidal locations. They measure in situ (shot resolved) the mass changes of eroded or deposited layers /1/ on top of a quartz crystal. This contribution reports in particular on the measurements from a QMB which was placed in the private flux region (PFR) below the supporting wedge of the Load Bearing Septum Replacement Plate (LBSRP) of the MKII-HD divertor with a direct view to the vertical tiles of the inner divertor, thus representing somewhat the geometrical situation in the inner divertor of ITER.

### **2. Experimental**

The QMB was positioned beneath the divertor tile 5, the LBSRP (divertor tile 5) and behind the protection tile between the LBSRP and tile 4, the inner base plate, as shown in figure 1. An aperture in the protection tile provides an open view to the inner divertor plasma and the inner vertical target. The quartz is oriented parallel to the magnetic field lines and recessed by 4.5 cm from the front surface of the protection tile such that only neutrals can contribute to the erosion/deposition processes. In this special QMB unit (no shutter) the crystal surface is continually exposed during JET operations and therefore measures the integral effect of a full plasma discharge. A frequency resolution of  $\pm 3$  Hz is achieved under the JET conditions,

corresponding to a thickness of approximately one monolayer for typical redeposited layers with densities of about  $1\text{g/cm}^3$ . The sensitivity is  $4.4 \times 10^{14} \text{C}_{\text{at}}/\text{Hz cm}^2$ . The measuring method



and use of QMBs in other fusion devices is explained more in detail in [2,3,4]. Since the frequency depends not only on mass but also on temperature, a second quartz crystal is placed in the QMB housing and protected from plasma impact to separate deposition from thermal effects. Thermal equilibrium of both crystals is a necessary condition for a

reliable measurement.

### 3. Results and Discussion

The measurements were carried out during the JET restart in 2005 (pulse no's 64300 - 65697) within a total divertor plasma time of about 16100 sec. Throughout this period in most of the discharges the QMB crystals did not reach thermal equilibrium on a shot by shot basis due to the high plasma pulse repetition rate and the lack of a shutter of this QMB-system. Therefore the data

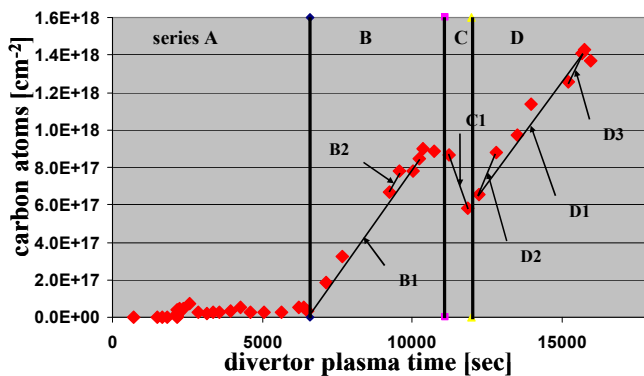


figure 2: erosion/deposition behaviour of a carbon layer in the private flux region of the MKII-HD divertor of JET

were selected such that the thermal equilibrium of the QMB system was verified which excluded for most cases a shot by shot analysis. Instead the data represent the layer erosion/deposition integrated over a series of discharges between two neighbouring measure points where thermal equilibrium is reached, mostly in the morning before plasma

operation has been started. The measured areal mass density of the carbon layer is plotted in figure 2 as a function of the divertor plasma time. The inner strike point was changed throughout the commissioning campaign for tile cleaning purposes with about 10 different combinations of strike point positions and sweeps. Nevertheless the inner strike point position during the shot

series marked B and D in figure 2 was predominantly on tile 3. This tile is located in line of sight with the quartz crystal, see figure 1. For the series A and C the strike point was mostly on tile 4, the base plate, with no or little direct line of sight with the quartz. The erosion and deposition behaviour in figure 2 shows a clear correlation to the location of the strike point with layer deposition during the shot series B and D and erosion during the C series. No significant mass change was measured during series A since no carbon layer was on the quartz at this time. From these data erosion/deposition rates normalized to divertor time were deduced for the series and sub series as marked in figure 2. They are listed in table 1. During the shot sequence B1, lasting 3851 sec, only low powered L-mode discharges were applied with about 2-3 MW ICRH,

shot series	strike point (SP) position	divertor plasma time [sec]	erosion/deposition [Catoms/cm <sup>2</sup> sec]	ELMS
B1	SP on tile 3 + sweeps tile 1, tile 3	3851	$2.3 \times 10^{14}$	no ELMS
B2	SP fixed on tile 3	330	$3.5 \times 10^{14}$	no ELMS
C1	SP on tile 4 + sweeps tile 1	622	$-4.6 \times 10^{14}$	no ELMS
D1	SP on tile 3 + sweeps tile 1, tile 3	3885	$2.2 \times 10^{14}$	partly ELMS
D2	SP fixed on tile 3	573	$3.9 \times 10^{14}$	mostly no ELMS
D3	SP on tile 3 + sweeps on tile 1, tile 3	451	$3.4 \times 10^{14}$	ELMS

Table 1:

some LH heating and only NBI blips. These conditions lead to a carbon deposition rate of  $2.3 \times 10^{14}$  Catom/sec cm<sup>2</sup>. B2 is a sub sequence of B1, with a duration of 330 sec for which the inner strike point was always fixed on tile 3. This shot sequence showed a deposition rate of  $3.5 \times 10^{14}$  Catom/sec cm<sup>2</sup>. During C1 the strike point was mainly on tile 4 with a total duration of 622 sec. Under these conditions the layer was eroded with a high rate of  $-4.6 \times 10^{14}$  Catom/sec cm<sup>2</sup>. The plasma conditions were comparable to the sequence B with mainly low power L mode, ELM-free discharges. Returning with the strike point to tile 3 during the sequence D1, the erosion behaviour turned again into deposition with an averaged rate of  $2.2 \times 10^{14}$  Catom/sec cm<sup>2</sup>. The deposition rate is comparable to the sequence B1 although the plasma input power steadily increased during this sequence leading also to Elmy H mode operation. Nevertheless no obvious increase of the deposition rate can be recognised in the averaged deposition behaviour. It should be noted that a remarkable amount of swept shots are also included in these series of discharges and also occasional operation on tile 4 which leads to erosion as discussed above. The deposition/erosion rates discussed above are averaged over the whole plasma divertor time which last typically about 25 sec with a wide time spread of low power additional ICRH and LH

heating. Four successive Elmy-H mode shots with an H mode phase of 3.5 sec and 12 MW input power could be identified ( 65617-65620) where thermal equilibrium was established. They show a reproducible deposition of  $1.2 \times 10^{16} \pm 4.4 \times 10^{14} \text{ C}_{\text{at}} / \text{cm}^2$  for each shot during a total time of about 25 sec yielding an averaged deposition rate of about  $4.4 \times 10^{14} \text{ C}_{\text{at}} / \text{sec cm}^2$  which must be compared with the averaged deposition of  $3.5 \times 10^{14} \text{ C}_{\text{at}} / \text{sec cm}^2$  for L mode operation with fixed strike point position on tile 3. Thus a pronounced additional deposition during the H mode phase could also not be identified in those selected shots at that location in the PFR. The expected strong effect of the 3.5 second ELM phase is probably diluted by the  $\sim 21$  second L-mode phase.

### 3. Summary and conclusions

With the plasma operated predominantly on the vertical targets, the private flux region of JET which faces the inner divertor target is a deposition dominated region. Under L mode low power heating conditions (mainly ICRH and LH) the mean deposition rate is about  $2.3 \times 10^{14} \text{ C}_{\text{at}} / \text{sec cm}^2$  whereas  $3.5 \times 10^{14} \text{ C}_{\text{at}} / \text{sec cm}^2$  were found during the sub series B2 with fixed strike point exclusively on tile 3. This indicates that under the given conditions strong sweeping with drastic changes in geometry reduces or compensates the deposition. No obvious strong increase of the deposition has been recognised in the series D with increasing the heating power leading to H mode operation. However only data averaged over daily operation have been analysed here in detail and further analysis on the influence of ELMS on the deposition is underway. With the plasma operating on the horizontal target, the inner PFR region turns into an erosion dominated area with an erosion of about  $-4.6 \times 10^{14} \text{ C}_{\text{at}} / \text{sec cm}^2$ . The data show again that the erosion/deposition is a complex competitive process under conditions of carbon deposition and re-erosion by neutral fluxes of hydrogen. In line with previous observations /5/, the geometric location of the strike point with respect to the location of the QMB-crystal plays a key role for the local erosion/deposition behaviour and supports the general behaviour of line of sight transport of eroded species.

### 4. References

- /1/ J.P. Coad et al., J. Nucl. Mater. 290–293 (2001), p. 224
- /2/ H.G. Esser et al. Fusion Engineering and Design Vol. 66-68, September 2003, Pages 855-860
- /3/ V. Rohde et al. Journal of Nuclear Materials Volumes 290-293, March 2001, Pages 317-320
- /4/ C.H. Skinner et al. Journal of Nuclear Materials Vol. 363-365, 15 June 2007, Pages 247-251
- /5/ H.G. Esser et al. Journal of Nuclear Materials Volumes 337-339, 1 March 2005, Pages 84-88